First-principles study of vibrational and dielectric properties of C_3N_4 polymorphs

G.-M. Rignanese, J.-C. Charlier, and X. Gonze
Unité de Physico-Chimie et de Physique des Matériaux, Université Catholique de Louvain, 1 Place Croix du Sud, B-1348 Louvain-la-Neuve, Belgium
and Research Center on Microscopic and Nanoscopic Materials and Electronic Devices (CERMIN), Université Catholique de Louvain, B-1348 Louvain-la-Neuve, Belgium

(Received 12 August 2002; published 27 November 2002)

Using the density-functional perturbation theory, the vibrational and dielectric properties are calculated for five C_3N_4 crystalline phases. The vibrational frequencies are found to differ significantly from one phase to another, thus giving a strong support to the use of Raman scattering and infrared absorption spectroscopy to identify the crystalline phase synthesized experimentally among the various polymorphs predicted theoretically. On the one hand, our findings raise serious doubts about the identification of the β-C_3N_4 phase in several experimental studies. On the other hand, our results will help to determine the atomic bonding configuration in amorphous carbon nitride.

DOI: 10.1103/PhysRevB.66.205416 PACS number(s): 78.30.−j, 63.20.−e, 77.22.−d

Fifteen years ago, Cohen[1] proposed carbon nitride (CN) as a superhard material[2] based on the expected short C-N bond length. Using first-principles calculations, hypothetical crystalline phases were successively proposed: β-C_3N_4,[3] defect zinc-blende cubic-C_3N_4,[4] α-C_3N_4,[5] and cubic-C_3N_4.[6] Their structural parameters were calculated and their bulk moduli B were predicted to be 427, 425, 425, and 496 GPa, respectively. A graphitic-C_3N_4 phase was also investigated.[4] It was found to be the most energetically-favorable structure, but its bulk modulus was predicted to be very low ($B = 51$ GPa). Another theoretical study was dedicated to carbon nitride compounds,[7] suggesting the use of nuclear magnetic resonance for sample characterizations.

Following the pioneering work of Ref. 1, considerable experimental efforts have been dedicated to the synthesis and the characterization of CN.[8–26] Nanometer to micrometer-sized crystals were found[13–22] usually embedded in an amorphous carbon nitride (a-CN_x) matrix.

Besides its predicted hardness, carbon nitride (even a-CN_x with a N/C ratio smaller than for C_3N_4) exhibit very interesting properties such as low friction coefficient, chemical inertness, and controllable electrical conductivity and optical band gap (by tuning its composition).[24] Consequently, CN is also considered to be very promising in the fields of tribological and wear-resistant coating, optical and electronic engineering.

Due to the small size of the crystallites obtained in experiments, a complete structural determination requires the combination of various experimental techniques. Among these, Raman scattering and infrared (IR) absorption spectroscopy are considered be very powerful tools. These methods are sensitive to slight variation in the lattice symmetry, and can be focused on a microscopic region. They have been widely used to characterize both the crystalline[19–22] and amorphous[23–26] phases of CN. However, in order to identify the different crystalline phases, their vibrational properties must be known *a priori*. Similarly, for the amorphous phases, it is not always straightforward to assign the vibrational frequencies to a given atomic bonding configuration.

The characterizations conducted[19–26] so far have relied on a simple qualitative approach[10] to estimate the vibrational frequencies of C_3N_4 phases through Hooke's law based on those of the equivalent phases of Si_3N_4. But a reliable theoretical prediction for all C_3N_4 crystalline polymorphs is still lacking and therefore requested by the experimental community.[19]

In this work, we use first-principles calculations to compute the phonon frequencies at the center of the Brillouin zone for five C_3N_4 crystalline polymorphs. Our calculations demonstrate that the vibrational frequencies differ significantly from one phase to another, allowing for a clear identification through Raman scattering and IR absorption spectroscopy. The phonon spectra of β-Si_3N_4 is also determined from first-principles in excellent agreement with experimental data. The comparison of the Raman peaks calculated for β-C_3N_4 and those for β-Si_3N_4 clearly proves that the simple model suggested in Ref. 10 does not hold, raising serious suspicions about the claims of several experimental studies. For all our C_3N_4 crystalline models, we present the Born effective charge tensors, and the dielectric permittivity tensors that are also calculated *ab initio*.

We consider the five most relevant C_3N_4 crystalline polymorphs: α-C_3N_4, β-C_3N_4, defect zinc-blende cubic-C_3N_4, cubic-C_3N_4, and graphitic-C_3N_4. The atomic coordinates and the cell parameters of all structures are fully relaxed within the local-density approximation to density-functional theory, as implemented in the ABINIT package.[27]. The exchange-correlation energy is evaluated using Perdew-Wang's parametrization[28] of Ceperley-Alder electron-gas data.[29] Only valence electrons are explicitly considered, and norm-conserving nonlocal pseudopotentials are used to account for the core-valence interactions.[30] The wave functions are expanded in plane waves up to a kinetic energy cutoff of 30 Ha and the k-point sampling for the various phases is chosen sufficiently high to insure convergence of all the calculated properties.

The space groups of the five crystals are indicated in Table I, as well as the calculated equilibrium structural parameters. The agreement with previous theoretical calculations[3–6] is very good.

TABLE I. Space groups, equilibrium structural parameters, dielectric constants, and Born effective charge tensors calculated for five C_3N_4 crystalline polymorphs.

	α	β	Defect zinc-blende	Cubic	Graphitic
Sym.	$P3_1c$ (159)	$P6_3/m$ (176)	$P\bar{4}3m$ (215)	$I\bar{4}3d$ (220)	$P\bar{6}m2$ (187)
a (Å)	6.4136	6.3540	3.3988	5.3662	4.7118
c (Å)	4.6704	2.3849			6.0957
C_1	(0.5170, 0.0810, 0.2100)	(0.2271, 0.8217, 0.7500)	(0.5000, 0.0000, 0.5000)	(0.8750, 0.0000, 0.2500)	(0.3509, 0.1754, 0.0000)
C_2	(0.1657, 0.2548, 0.9999)				(0.0190, 0.5095, 0.5000)
N_1	(0.0000, 0.0000, 0.0000)	(0.3333, 0.6667, 0.7500)	(0.2549, 0.2549, 0.2549)	(0.2838, 0.2838, 0.2838)	(0.0000, 0.0000, 0.0000)
N_2	(0.3333, 0.6667, 0.6362)	(0.0331, 0.3303, 0.2500)			(0.6667, 0.3333, 0.5000)
N_3	(0.3470, 0.9505, 0.9796)				(0.1705, 0.3409, 0.5000)
N_4	(0.3147, 0.3189, 0.2517)				(0.5037, 0.4963, 0.0000)
ϵ_∞	(5.03 5.03 4.91)	(5.15 5.15 4.73)	5.21	5.59	(6.15 6.15 2.84)
ϵ_0	(7.01 7.01 6.90)	(7.81 7.81 6.13)	7.37	8.37	(8.82 10.34 2.92) [a]
Z^*_{C1}	$\begin{pmatrix} 1.87 & 0.32 & -0.01 \\ 0.26 & 2.34 & 0.14 \\ 0.10 & 0.08 & 2.05 \end{pmatrix}$	$\begin{pmatrix} 2.71 & 0.00 & 0.00 \\ 0.05 & 2.13 & 0.00 \\ 0.00 & 0.00 & 1.99 \end{pmatrix}$	$\begin{pmatrix} 2.76 & 0.00 & 0.00 \\ 0.00 & 1.68 & 0.00 \\ 0.00 & 0.00 & 1.68 \end{pmatrix}$	$\begin{pmatrix} 2.30 & 0.12 & 0.00 \\ -0.12 & 2.30 & 0.00 \\ 0.00 & 0.00 & 2.55 \end{pmatrix}$	$\begin{pmatrix} 3.69 & 1.01 & 0.00 \\ 1.01 & 2.52 & 0.00 \\ 0.00 & 0.00 & 0.51 \end{pmatrix}$
	[+1.73 +2.51 +2.02]	[+2.72 +2.13 +1.99]	[+2.76 +1.68 +1.68]	[+2.30 +2.30 +2.55]	[+4.28 +1.94 +0.51]
Z^*_{C2}	$\begin{pmatrix} 2.23 & -0.22 & 0.36 \\ -0.19 & 2.15 & 0.03 \\ 0.52 & -0.11 & 2.28 \end{pmatrix}$				$\begin{pmatrix} 3.61 & 1.02 & 0.00 \\ 1.02 & 2.43 & 0.00 \\ 0.00 & 0.00 & 0.66 \end{pmatrix}$
	[+2.14 +2.75 +1.78]				[+4.20 +1.84 +0.66]
Z^*_{N1}	$\begin{pmatrix} -1.91 & 0.17 & 0.00 \\ -0.17 & -1.91 & 0.00 \\ 0.00 & 0.00 & -0.95 \end{pmatrix}$	$\begin{pmatrix} -2.23 & 0.25 & 0.00 \\ -0.25 & -2.23 & 0.00 \\ 0.00 & 0.00 & -1.11 \end{pmatrix}$	$\begin{pmatrix} -1.53 & 0.12 & 0.12 \\ 0.12 & -1.53 & 0.12 \\ 0.12 & 0.12 & -1.53 \end{pmatrix}$	$\begin{pmatrix} -1.79 & -0.28 & 0.42 \\ -0.42 & -1.79 & -0.28 \\ 0.28 & -0.42 & -1.79 \end{pmatrix}$	$\begin{pmatrix} -2.98 & 0.00 & 0.00 \\ 0.00 & -2.98 & 0.00 \\ 0.00 & 0.00 & -0.48 \end{pmatrix}$
	[−1.91 −1.91 −0.95]	[−2.23 −2.23 −1.11]	[−1.65 −1.30 −1.65]	[−2.14 −2.14 −1.09]	[−2.98 −2.98 −0.48]
Z^*_{N2}	$\begin{pmatrix} -1.85 & -0.12 & 0.00 \\ 0.12 & -1.85 & 0.00 \\ 0.00 & 0.00 & -1.31 \end{pmatrix}$	$\begin{pmatrix} -1.86 & -0.59 & 0.00 \\ -0.47 & -1.49 & 0.00 \\ 0.00 & 0.00 & -1.62 \end{pmatrix}$			$\begin{pmatrix} -2.91 & 0.00 & 0.00 \\ 0.00 & -2.91 & 0.00 \\ 0.00 & 0.00 & -0.62 \end{pmatrix}$
	[−1.85 −1.85 −1.31]	[−2.24 −1.12 −1.62]			[−2.91 −2.91 −0.62]
Z^*_{N3}	$\begin{pmatrix} -1.67 & -0.32 & 0.18 \\ -0.32 & -1.47 & -0.17 \\ 0.05 & -0.33 & -1.72 \end{pmatrix}$				$\begin{pmatrix} -3.07 & 0.00 & 0.00 \\ 0.00 & -1.09 & 0.00 \\ 0.00 & 0.00 & -0.44 \end{pmatrix}$
	[−1.81 −1.11 −1.93]				[−3.07 −1.09 −0.44]
Z^*_{N4}	$\begin{pmatrix} -1.48 & -0.17 & -0.23 \\ -0.25 & -1.47 & 0.11 \\ -0.28 & 0.26 & -1.87 \end{pmatrix}$				$\begin{pmatrix} -1.59 & -0.86 & 0.00 \\ -0.86 & -2.58 & 0.00 \\ 0.00 & 0.00 & -0.36 \end{pmatrix}$
	[−1.13 −1.68 −2.01]				[−3.08 −1.10 −0.36]

[a]See Ref. 31.

TABLE II. Calculated phonon frequencies of α-C_3N_4 (in cm^{-1}) with their symmetry assignments.

Infrared							
$A1$(TO)	375.7	421.0	477.0	546.4	672.6	797.3	922.0
	1000.5	1051.2	1108.1	1159.1	1232.9	1380.7	
$A1$(LO)	375.9	421.8		548.6	679.2	799.0	
		1063.4		1225.0	1341.7	1381.0	
E(TO)	335.4	396.7	482.1	545.2	587.4	600.9	644.0
	690.6	719.0	788.8	830.3	895.0	937.8	1008.6
	1029.3	1076.5	1082.1	1097.2	1118.4	1145.9	1153.0
	1179.9	1203.8	1245.2	1256.2	1289.4	1372.8	
E(LO)	335.5		482.2		587.4	601.4	
	694.8	721.6		833.3		946.3	1021.4
	1033.9		1087.6	1098.5	1118.6	1155.7	
	1187.0	1227.7		1285.3	1346.2	1394.1	
Silent							
$A2$	400.1	523.5	608.5	712.2	739.6	848.9	888.7
	934.1	1043.5	1065.2	1157.3	1197.6	1240.1	1295.0

The dynamical and dielectric properties (phonon frequencies at the zone center, Born effective charge tensors, and dielectric tensors) are then computed as second-order derivatives of the total energy with respect to an external electric field or to atomic displacements. These second-order derivatives are obtained within a variational approach to density-functional perturbation theory,[27,32–34] also implemented in the ABINIT package. We used the same parameters as for the calculation of the structural properties. We also performed tests which proved the associated numerical accuracy to be excellent. We report in Table I the dielectric tensors and the Born effective charge tensors (the principal values of their symmetric is indicated between brackets).

The dielectric properties of CN have not been studied very much experimentally. We are only aware of the measurement of the dielectric constant of a-CN_x films[35] in which a value of $\epsilon_\infty \simeq 5.5$ has been reported for $x = 25\%$. Our calculated values in Table I are in very reasonable agreement with this experiment. For comparison, Corkill and Cohen[36] proposed a rough estimate of 5.25 for β-C_3N_4, whereas in Ref. 37 a value of 3.8 has been calculated (this low value is probably due to the fact that local field effects were not included). As expected, the biggest value of ϵ_∞ is reached for the systems with sp^2-bonded C atoms (for the in-plane component). For the systems with sp^3-bonded C atoms, the highest value is reached for cubic-C_3N_4 which is also the system with the highest bulk modulus. Similar conclusions hold for the static dielectric constant ϵ_0.

The Born effective charge tensors Z^* also present a very different behavior in the case of systems with sp^3 or sp^2-bonded C atoms. In the former case, the tensors are quite isotropic with average principal values of $Z_C^* \simeq +2.3$ and $Z_N^* \simeq -1.7$. In the latter case, the tensors are very anisotropic with bigger in-plane principal values (up to $+4$ for C and -3 for N) and very small principal values perpendicularly to the plane. Note also that the N atoms that are threefold coordinated ($N1$and $N2$) present an homogeneous principal value in the plane, while there are two well separated values for those that are twofold coordinated ($N3$ and $N4$). Finally, the signs of the Born effective charge tensors reflect the difference in electronegativity between C and N atoms.

The calculated phonon frequencies (including LO-TO splitting) and their symmetry assignments are given for the five polymorphs in Tables II–VI.[31] In Fig. 1, we present the calculated IR absorption spectra for the five crystalline

TABLE III. Calculated phonon frequencies of β-C_3N_4 (in cm^{-1}) with their symmetry assignments.

Raman					
Ag	442.1	637.1	1080.3	1290.3	
$E1g$	411.9	1196.9			
$E2g$	304.4	718.0	890.7	1148.9	1377.5
Infrared					
Au(TO)	513.6	1215.4			
Au(LO)	517.6	1372.6			
$E1u$(TO)	583.2	947.9	1130.5	1324.7	
$E1u$(LO)	586.7	1014.0	1204.9	1422.6	
Silent					
Bg	429.8	701.3	1110.8		
Bu	199.3	921.1	1024.7	1390.0	
$E2u$	599.1	1134.0			

TABLE IV. Calculated phonon frequencies of defect zinc-blende C_3N_4 (in cm^{-1}) with their symmetry assignments.

Raman			
$A1$	990.5		
E	1103.7		
Infrared			
$T2$(TO)	738.3	1036.4	1254.5
$T2$(LO)	752.8	1159.8	1308.0
Silent			
$T1$	741.8	828.9	

TABLE V. Calculated phonon frequencies of cubic C_3N_4 (in cm^{-1}) with their symmetry assignments.

Raman					
$A1$	447.2				
E	699.5	941.5	1193.2		
Infrared					
$T2$(TO)	531.1	581.1	918.5	1059.4	1250.6
$T2$(LO)	531.4		923.5	1247.7	1291.9
Silent					
$A2$	852.0	1060.8			
$T1$	680.8	820.3	956.8	1091.4	1131.9

polymorphs[31] as well as the theoretical positions of the Raman peaks.[38]

From Fig. 1, it appears that the five crystalline phases can easily be distinguished both by their Raman and IR vibrational frequencies. This gives a strong support to the use of Raman scattering and IR absorption spectroscopy to identify the C_3N_4 crystallites synthesized experimentally among the various polymorphs of predicted theoretically. The calculated frequencies should also help to assign the measured peaks in a-CN_x in terms of the underlying atomic bonding configuration.

So far, the Raman peaks for C_3N_4 have been estimated based on those of Si_3N_4 through a simple qualitative approach. It consists in correlating the stretching frequency for the C-N bond to the Si-N bond through Hooke's law:

$$\rho=\frac{\nu_{C_3N_4}}{\nu_{Si_3N_4}}=\sqrt{\frac{B_{C_3N_4}d_{CN}u_{Si_3N_4}}{B_{Si_3N_4}d_{SiN}u_{C_3N_4}}}, \tag{1}$$

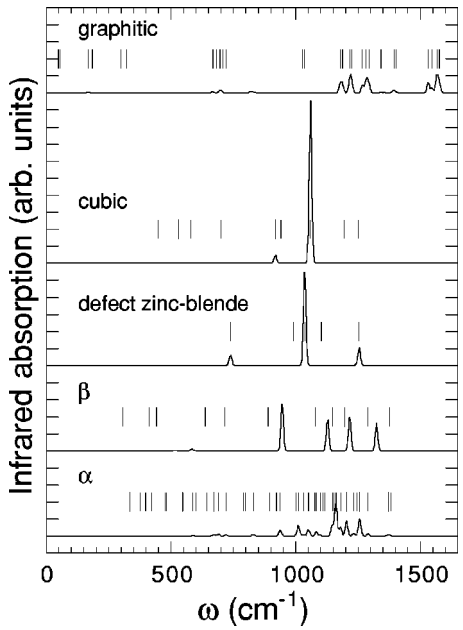

FIG. 1. Infrared absorption spectra for the different C_3N_4 polymorphs (Ref. 31). The Raman frequencies (vertical lines) are also indicated (Ref. 38).

TABLE VI. Calculated phonon frequencies of graphitic C_3N_4 (in cm^{-1}) with their symmetry assignments (Ref. 31).

		TO	LO-x	LO-y	LO-z
Raman					
$A1'(1)$	1057.2	1028.2	1028.2	1028.2	1028.2
$A1'(2)$	1061.3	1034.2	1034.2	1034.2	1034.2
$A1'(3)$	1375.9	1394.8	1401.5	1397.2	1394.8
$A1'(4)$	1391.9	1402.7	1407.3	1402.9	1402.7
$E''(1)$	231.3i	168.8	169.4	180.6	168.8
		184.5	184.5	185.4	184.6
$E''(2)$	258.5i	298.5	301.4	298.8	298.5
		323.1	323.1	323.1	323.1
$E''(3)$	702.4	695.7	696.0	696.0	696.9
		697.4	699.7	706.9	697.5
$E''(4)$	718.0	708.7	709.9	709.3	708.7
		720.9	721.0	721.0	720.9
Infrared					
$A2''(1)$	131.5	133.6	133.7	133.7	133.6
$A2''(2)$	467.9	465.9	465.9	466.2	465.9
$A2''(3)$	474.2	474.1	474.1	474.1	474.4
$A2''(4)$	800.2	819.5	819.5	819.5	832.0
$A2''(5)$	830.1	832.6	833.0	834.0	836.0
$E'(1)$	54.9	47.3	47.3	47.6	47.5
		54.8	54.9	54.9	54.8
$E'(2)$	698.4	666.8	667.9	667.5	666.8
		668.2	669.3	668.4	668.2
$E'(3)$	700.6	680.7	680.8	680.7	681.4
		684.3	684.4	684.5	684.5
$E'(4)$	1098.3	1178.9	1182.5	1180.8	1178.9
		1187.3	1198.3	1189.7	1187.3
$E'(5)$	1112.6	1217.6	1220.9	1221.2	1217.7
		1224.2	1236.5	1242.1	1224.5
$E'(6)$	1323.2	1267.4	1268.5	1274.0	1267.5
		1281.0	1281.3	1285.3	1281.3
$E'(7)$	1330.5	1293.9	1339.0	1332.9	1293.9
		1341.5	1342.7	1345.3	1342.5
$E'(8)$	1540.4	1531.4	1539.7	1533.7	1531.4
		1546.6	1556.4	1547.5	1546.6
$E'(9)$	1560.0	1566.4	1572.7	1572.1	1567.6
		1575.7	1619.3	1645.9	1578.0
Silent					
$A2'(1)$	436.4	465.4	465.5	465.6	465.5
$A2'(2)$	442.8	469.5	469.6	469.5	469.5
$A2'(3)$	1329.8	1286.1	1290.1	1292.6	1286.1
$A2'(4)$	1341.7	1354.5	1354.6	1355.8	1356.5

where B is the bulk modulus, d is the bond length, and u is the reduced mass. This method has essentially been used for the β phase,[19–22] but also for the α phase,[19,22] mostly on the Raman modes.

In order to test the quality of this approximation, we also perform first-principles calculations of the vibrational properties for β-Si_3N_4. In Table VII, we present our calculated Raman frequencies for β-Si_3N_4 and for β-C_3N_4. For silicon nitride, we also report the experimental data,[40,41] as well as the results of a previous theoretical work.[42]

TABLE VII. Comparison of the calculated Raman spectra of β-C_3N_4 and β-Si_3N_4 with their scale factor ρ as defined by Eq. (1). The frequencies are expressed in cm^{-1}.

	β-Si_3N_4			β-C_3N_4	ρ
	Expt.[a]	Theor.[b]	This work	This work	This work
$E_{2g}(1)$	185	183	180.1	304.4	1.69
$A_g(1)$	208	201	201.4	442.1	2.20
$E_{1g}(1)$	230	228	222.8	411.9	1.85
$E_{2g}(2)$	452	444	446.8	718.0	1.61
$A_g(2)$		457	459.9	637.1	1.39
$E_{2g}(3)$	620	603	614.2	890.7	1.45
$A_g(3)$	733	715	728.7	1080.3	1.48
$E_{1g}(2)$	866	836	863.1	1196.9	1.39
$E_{2g}(4)$	930	897	926.5	1148.9	1.24
$A_g(4)$	940	908	936.1	1290.3	1.38
$E_{2g}(5)$	1048	1012	1041.6	1377.5	1.32

[a]Experimental values (Refs. 40 and 41).

[b]Results of a previous theoretical calculation (Ref. 42).

Our calculated phonon frequencies present a rms absolute deviation of 5.5 cm^{-1}, and a rms relative deviation of 1.5% with respect to the measurements of Refs. 41 and 40. For comparison, the corresponding rms absolute (relative) deviations are 23.7 cm^{-1} (2.9%) for the previous calculation.[42] This is an excellent agreement with both experiments and theory, and makes us very confident in the predictions for the C_3N_4 phases.

In Table VII, we also report the calculated scale factor ρ between the Raman frequencies of β-C_3N_4 and β-Si_3N_4. In experimental studies,[19–22] a value of 1.43–1.47 has been estimated for ρ by substituting the theoretical values of the various parameters in Eq. (1) as proposed in Ref. 10. From our calculations, we confirm that the model of Eq. (1) works only for the stretching modes $A_g(2)$–(4), $E_{1g}(2)$, and $E_{2g}(3)$. For the other modes, the calculated value of ρ differs significantly from 1.43–1.47, especially in the low-frequency range [up to 50% difference for $A_g(1)$], where bending modes are predominant.

These results raise serious doubts about the conclusions of some experimental studies.[19–22] In the Raman spectrum of β-Si_3N_4,[40–42] the three lowest frequency modes (E_{2g}, A_g, and E_{1g}) at 185, 208, and 230 cm^{-1} are very pronounced, and can therefore be used as a spectral signature. This observation has been exploited to identify the β-C_3N_4, crystalline phase in experiments.

Based on Eq. (1), these three peaks have been predicted to be at 266, 300, and 327 cm^{-1}. Experimentally,[19–22] three intense bands have been observed at about the same frequencies, leading some of the authors[20–22] to claim the identification of β-C_3N_4, though the measured spectra differ quite significantly from one experiment to another. Moreover, a lower frequency Raman peak has also been reported in a few cases: 199 cm^{-1} in Ref. 19 or 220 cm^{-1} in Ref. 21. It has been correlated with the A_g peak at 145 cm^{-1} observed in the experimental Raman spectra of β-Si_3N_4 (Ref. 41). In view of our predictions for the Raman peak positions, we have several concerns regarding the interpretation of these experiments.

First, regarding this low-frequency peak, we would like to confirm the results of Ref. 42. For β-Si_3N_4, our calculations show that the A_g mode is located at 459.9 cm^{-1} in excellent agreement with the value of 457 cm^{-1} calculated in Ref. 42, while *no* A_g mode is found in the spectral region near 145 cm^{-1}. Hence for β-C_3N_4, the experimental peaks measured around 200 cm^{-1} should not be correlated with this peak even if the approximation suggested in Ref. 10 was working perfectly.

Second, in our first-principles calculations, the three lowest frequency Raman peaks are found at 305.0, 442.1, and 412.3 cm^{-1} for β-C_3N_4. These are quite different from the values of 266, 300, and 327 cm^{-1} predicted using Eq. (1). Therefore the assignment of the three intense bands that have been observed experimentally at about the same frequencies to the β-C_3N_4 phase[20–22] should be ruled out. In fact, even by comparing the whole experimental spectra to our calculated peaks, it is very difficult to reach a final conclusion about the presence or not of β-C_3N_4 in the samples.

Finally, we also would like to point out a consequence of the decrease of the scale factor ρ at higher frequency [modes E_{2g} (4) and (5)]. Indeed, the approximation of Ref. 10 has lead some authors to assign frequencies as high as 1480 cm^{-1} (Ref. 21) or 1539 cm^{-1} (Ref. 22) to Raman modes of β-C_3N_4. In our calculations, we find that the highest Raman vibrational frequency is at 1377.0 cm^{-1} for this phase. It is 1381 cm^{-1} for α-C_3N_4, 1254.5 cm^{-1} for defect zinc-blende cubic C_3N_4, and 1250.6 cm^{-1} for cubic C_3N_4. All these values are well below those reported in experiments, excluding the attribution of such high-frequency peaks to one of these phases. In contrast, for the graphitic-C_3N_4, the highest Raman mode is calculated to be 1560.0 cm^{-1}. This higher frequency can be understood in terms of the higher strength for the C-N bonds due to carbon sp^2 bonding compared to sp^3 for the other phases, this effect being further increased for the twofold coordinated N atoms by an extra reduction of the C-N bond length. This suggests that the high-frequency peaks of Refs. 21 and 22 could be attributed to the presence of twofold coordinated N atoms.

In conclusion, we have presented a first-principles study of the phonon frequencies at the center of the Brillouin zone for five C_3N_4 crystalline polymorphs. The calculated vibrational frequencies differ significantly from one phase to another. Consequently, we have demonstrated that Raman scattering and IR absorption spectroscopy can be used for a complete characterization of the CN crystalline samples. By comparing the calculated phonon spectra of β-C_3N_4 and β-Si_3N_4, we have shown that they cannot be correlated through a simple Hooke's law approximation, contrarily to what has been suggested previously and widely used in experiments in the absence of reliable theoretical references. Finally, the Born effective charge tensors, and the dielectric permittivity tensors have also calculated and compared between the five C_3N_4 crystalline models. We believe that our

theoretical predictions should be highly valuable for the experimental community in framework of the characterization of crystalline and amorphous carbon nitride.

The authors acknowledge support from the National Fund for Scientific Research (FNRS-Belgium), from the FRFC Project No. 2.4556.99 ''Simulations numériques et traitement des données,'' from the Belgian Program on Interuniversity Attraction Poles (PAI5/1/1) on ''Quantum Size Effects in Nano-structured Materials,'' and from the ''Action de Recherche Concertée'' sponsored by the ''Communauté Française de Belgique.''

[1] M. L. Cohen, Phys. Rev. B **32**, 7988 (1985).
[2] For a review article, see J. Haines, J. M. Léger, and G. Bocquillon, Annu. Rev. Mater. Res. **31**, 1 (2001).
[3] A. Y. Liu and M. L. Cohen, Science **245**, 841 (1989); Phys. Rev. B **41**, 10 727 (1990).
[4] A. Y. Liu and R. M. Wentzcovitch, Phys. Rev. B **50**, 10 362 (1994).
[5] Y. Guo and W. A. Goddard, III, Chem. Phys. Lett. **237**, 72 (1995).
[6] D. Teter and R. J. Hemley, Science **271**, 53 (1996).
[7] Y.-G. Yoon, B. G. Pfrommer, F. Mauri, and S. G. Louie, Phys. Rev. Lett. **80**, 3388 (1998).
[8] H. X. Han and B. J. Feldman, Solid State Commun. **65**, 921 (1988).
[9] T. Sekine, H. Kanda, Y. Bando, M. Yokohama, and K. Hojou, J. Mater. Sci. Lett. **9**, 1376 (1990).
[10] M. Wixom, J. Am. Ceram. Soc. **73**, 1973 (1990).
[11] L. Maya, D. R. Cole, and E. W. Hagaman, J. Am. Ceram. Soc. **74**, 1686 (1991).
[12] D. Marton, K. J. Boyd, A. H. Al-Bayati, S. S. Todorov, and J. W. Rabalais, Phys. Rev. Lett. **73**, 118 (1994).
[13] C. Niu, Y. Z. Lu, and C. M. Lieber, Science **261**, 334 (1993).
[14] K. M. Yu, M. L. Cohen, E. E. Haller, W. L. Hansen, A. Y. Liu, and I. C. Wu, Phys. Rev. B **49**, 5034 (1994).
[15] J. P. Rivière, D. Texier, J. Delafond, M. Jaouen, E. L. Mathe, and J. Chaumont, Mater. Lett. **22**, 115 (1995).
[16] Z. M. Ren, Y. C. Du, Y. Qiu, J. D. Wu, Z. F. Ying, X. X. Xiong, and F. M. Li, Phys. Rev. B **51**, 5274 (1995).
[17] L. P. Guo, Y. Chen, E. G. Wang, L. Li, and Z. X. Zhao, Chem. Phys. Lett. **268**, 26 (1997).
[18] J. Martin-Gil, F. J. Martin-Gil, M. Sarikaya, M. Qian, M. José-Yacamán, and A. Rubio, J. Appl. Phys. **81**, 2555 (1997).
[19] L. C. Chen, D. M. Bhusari, C. Y. Yang, K. H. Chen, T. J. Chuang, M. C. Lin, C. K. Chen, and Y. F. Huang, Thin Solid Films **303**, 66 (1997).
[20] T.-Y. Yen and C.-P. Chou, Appl. Phys. Lett. **67**, 2801 (1995); Solid State Commun. **95**, 281 (1995).
[21] P.-N. Wang, Z. Guo, X.-T. Ying, J.-H. Chen, X.-M. Xu, and F.-M. Li, Phys. Rev. B **59**, 13 347 (1999).
[22] Y. Zhang and Y. Gu, Philos. Mag. Lett. **81**, 505 (2001).
[23] J. H. Kaufman, S. Metin, and D. D. Saperstein, Phys. Rev. B **39**, 13 053 (1989).
[24] A. Bousetta, M. Lu, A. Bensaoula, and A. Schultz, Appl. Phys. Lett. **65**, 696 (1994).
[25] Y. F. Lu, Z. M. Ren, W. D. Song, D. S. H. Chan, T. S. Low, K. Gamani, G. Chen, and K. Li, J. Appl. Phys. **84**, 2909 (1998).
[26] Y. Aoi, K. Ono, and E. Kamijo, J. Appl. Phys. **86**, 2318 (1999).
[27] ABINIT is a common project of the Université Catholique de Louvain, Corning Incorporated, and other contributors (http://www.ABINIT.org). It relies on an efficient fast fourier transform algorithm (Ref. 43) for the conversion of wave functions between real and reciprocal space, on the adaptation to a fixed potential of the band-by-band conjugate gradient method (Ref. 44) and on a potential-based conjugate gradient algorithm for the determination of the self-consistent potential (Ref. 45). Technical details on the computation of responses to atomic displacements and homogeneous electric fields can be found in Ref. 33 while Ref. 34 presents the subsequent computation of dynamical matrices, Born effective charge tensors, dielectric permittivity tensors, and interatomic force constants.
[28] J. P. Perdew and Y. Wang, Phys. Rev. B **45**, 13 244 (1992).
[29] D. M. Ceperley and B. J. Alder, Phys. Rev. Lett. **45**, 566 (1980).
[30] N. Troullier and J. L. Martins, Phys. Rev. B **43**, 1993 (1991).
[31] The graphitic-C_3N_4 phase presents some unstable vibrational modes ($\omega \sim 300i$ cm^{-1}) in agreement with Ref. 39. Therefore the calculated frequencies, the IR absorption spectra, the Raman peak positions, and the static dielectric constant presented here correspond to a pseudographitic phase. This model structure is obtained by reducing the original $P\bar{6}m2$ to $P1$ and fully relaxing the structural parameters and the atomic positions. The other properties in Table I are for the original phase.
[32] X. Gonze, D. C. Allan, and M. P. Teter, Phys. Rev. Lett. **68**, 3603 (1992).
[33] X. Gonze, Phys. Rev. B **55**, 10 337 (1997).
[34] X. Gonze and C. Lee, Phys. Rev. B **55**, 10 355 (1997).
[35] F. Barreca, A. M. Mezzasalma, G. Mondio, F. Neri, S. Trusso, and C. Vasi, Phys. Rev. B **62**, 16 893 (2000).
[36] J. L. Corkill and M. L. Cohen, Phys. Rev. B **48**, 17 622 (1993).
[37] H. Yao and W. Y. Ching, Phys. Rev. B **50**, 11 231 (1994).
[38] The calculated Raman frequencies of β-C_3N_4 change by less than 6% when a pressure of ± 15 GPa is applied to the crystal structure (resulting in a volume variation of $\pm 4\%$). This gives an insight on the effect of the possible presence of residual strain in the synthesized samples.
[39] Y. Miyamoto, M. L. Cohen, and S. G. Louie, Solid State Commun. **102**, 605 (1997).
[40] N. Wada, S. A. Solin, J. Wong, and S. Prochazka, J. Non-Cryst. Solids **43**, 7 (1981).
[41] K. Honda, S. Yokoyama, and S. Tanaka, J. Appl. Phys. **85**, 7380 (1999).
[42] J. Dong and O. F. Sankey, J. Appl. Phys. **87**, 958 (2000).
[43] S. Goedecker, SIAM J. Sci. Comput. (USA) **18**, 1605 (1997).
[44] M. C. Payne, M. P. Teter, D. C. Allan, T. A. Arias, and J. D. Joannopoulos, Rev. Mod. Phys. **64**, 1045 (1992).
[45] X. Gonze, Phys. Rev. B **54**, 4383 (1996).